Egyptian Geophysical Society
EGS Journal, Vol. 16, No. 1, 145-158 (2018)

GEOPHYSICAL CHARACTERIZATION OF THE COASTAL AQUIFER WEST EL-QASR AREA, NORTHWESTERN COAST, EGYPT

H.H. MAHMOUD and M.S.M. BARSEEM

Geophysical Exploration Department, Desert Research Center, Cairo - Egypt

توصيف جيوفيزيائي للخزان الساحلي غرب منطقة القصر، الساحل الشمالي الغربي، مصر

الخلاصة: تم عمل مسح جيوفيزيقي سطحي غرب منطقة القصر بالساحل الشمالي الغربي لمصر لتوضيح الخصائص الجيوفيزيقية للخزان الساحلي. وتتميز منطقة الدراسة بوجود خزان الحجر الجيري البطروخي التابع لعصر البليستوسين والذي اختلط بماء البحر. ويمثل هذا الخزان المصدر الرئيسي للمياه الجوفية التي تستخدم في المشروعات الزراعية علي طول الشريط الساحلي.

تم التكامل بنجاح بين تقنيات المسح الجيوفيزيقي السطحي والتي تشمل الجسات الجيوكهربية الرأسية وبروفيلات المقاومة النوعية ثنائية الأبعاد والجسات الكهرومغناطيسية لتحديد الطبقات الحاملة للمياه وامتداداتها وتحديد طبقة الماء الآسن المناسبة للاستغلال بمنطقة الدراسة وتحديد عمق السطح الفاصل بين الماء الأسن والماء المالح في الخزان الساحلي. وأثبتت نتائج الجسات الكهرومغناطيسية نجاحا كبيرا في تتبع الحد الفاصل بين الماء الأسن والماء المالح بمنطقة الدراسة وأستخدمت قيم المقاومة النوعية الكلية للطبقة الحاملة للمياه تحت هذا الحد لحساب مسامية الخزان بتطبيق معادلة أرشي ووجد أن لهذا الخزان مسامية ممتازة (٣٣,٠ %).

الجمع بين طرق الجسات الجيوكهربية الرئسية وبروفيلات المقاومة النوعية ثنائية الأبعاد والجسات الكهرومغناطيسية بالإضافة إلي المعلومات المتاحة من الابار الموجودة بالمنطقة قادر علي تقليل الغموض أثناء تفسير البيانات الحقلية. وقد أقترح أنسب الأماكن لحفر آبار جديدة.

ABSTRACT: *A surface geophysical survey was performed west El-Qasr area, in the Northwestern Coast of Egypt, to clarify the geophysical characterization of the coastal aquifer. The study area is characterized by presence of Pleistocene oolitic limestone aquifer that is contaminated by sea water intrusion. This aquifer represents the main source of groundwater that used in agriculture projects along the coastal plain.*

The integration between surface geophysical techniques including Vertical Electrical Sounding (VES), Two-Dimensional Resistivity Imaging profiles (2-D) and Time Domain Electromagnetic Sounding (TDEM) are used successfully to determine water bearing layers and their spatial distribution, outline the brackish water bearing layer that is suitable for exploitation along the study area and to detect depth to brackish/saline water interface in the coastal aquifer. TDEM sounding is proven as a successful method to trace brackish/saline water interface in the study area; bulk resistivity of the water bearing layer below this interface was used to calculate the porosity of this aquifer by applying Archie's equation; this aquifer has an excellent porosity values (33.0 %).

The combination between VES, 2-D and TDEM methods beside the available information from the existing wells is able to decrease the ambiguity during the interpretation of the acquired data. Interpreted data of the surface geophysical tools exhibit a good match between them and the proper sites for drilling new wells are recommended.

1. INTRODUCTION

Nowadays there is a great attention for the northwestern coast of Egypt due to its great environmental, economic and social relevance. This area depends mainly on rainfall for agriculture activities during winter months while the groundwater is used as a supplementary irrigation source during summer months. Rainfall precipitation is the only source for drinking in the tableland area where it recharges the shallow aquifers or it can be stored in the manmade cisterns. Therefore, suitable monitoring and protection actions are fundamental for preservation of the groundwater. Many challenges are faced this area from the impacts of climate changes represented in changes in sea level and precipitation. The costal aquifer along the northwestern coast is affected by sea water intrusion, which is the main problem in this arid region that leading to land desertification (Khalil et al., 2013; Soliman et al., 2013; Massoud et al., 2015 and Eissa et al., 2016).

The study area is located along the Northwestern Coast of Egypt; it located to the west from El Qasr Village west Marsa Matruh City by 12 km. This area is bounded by latitudes 31° 20' 18" and 31° 22' 33" N and longitudes 27° 4'and 27° 7' E (Fig. 1); it covers an area of about 20 km^2. It characterized by arid climate where the annual rainfall does not exceed 154 mm (El Sabri et al., 2011), relative humidity is high in July (73%) and it is moderate in March (63 %). Evaporation intensity varies between 162 mm in summer and 28 mm in winter, air temperature is relatively mild in summer (26.8 ºC) and it is low in winter (12.8 ºC).

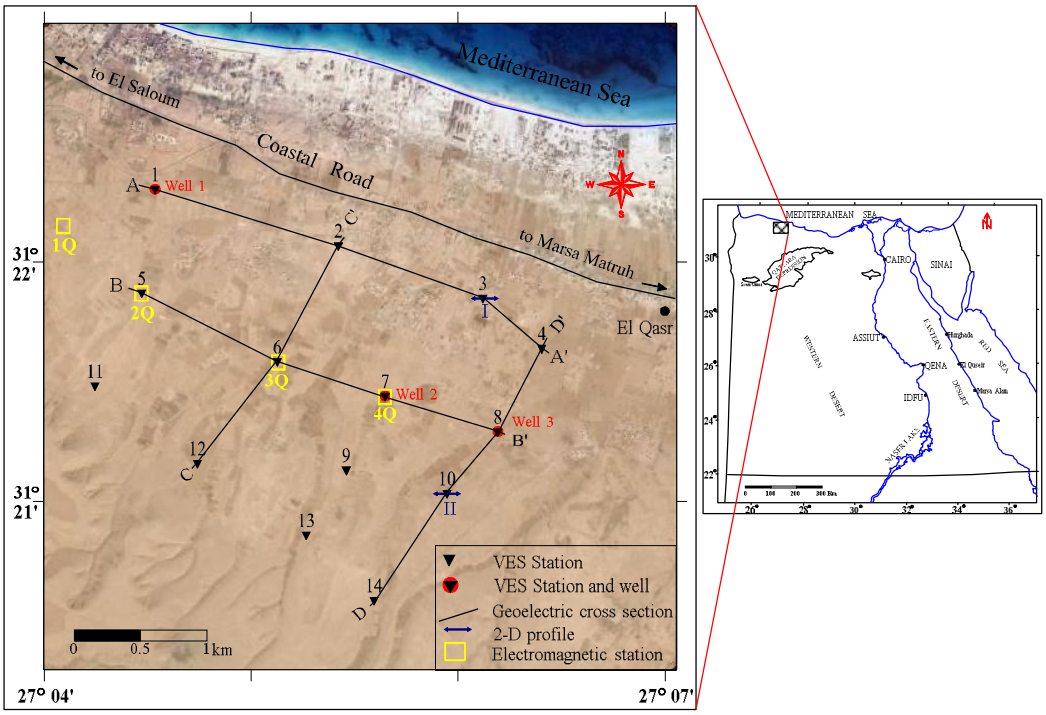

Fig. 1: Location map of the study area.

The present work aims to determine the geophysical characterization of the coastal aquifer and the effect of sea water intrusion in the study area, it includes detecting the water bearing layers and their horizontal and vertical extensions, outline the brackish water layer that is suitable for exploitation, trace brackish/saline water interface, estimate porosity of the aquifer and determine the proper site for drilling new wells by applying Vertical Electric Sounding (VES), Two-dimensional resistivity imaging (2-D) and Time domain Electromagnetic (TDEM) soundings.

2- GEOLOGIC BACKGROUND

The coastal area is characterized by low relief and mild topography. It is distinguished into three main geomorphic units including the coastal plain, the piedmont plain and the structural tableland. The coastal plain runs parallel to the Mediterranean Sea; it extends inland southward. The landscape in the coastal plain is characterized by a number of elongate ridges which form gentle sweeping curves running sub-parallel to the present Mediterranean coast. It displays different morphologic features along the different localities due to the influence of local structural, lithologic, and physiographic conditions like foreshore dunes, coastal ridge and coastal depressions (Mohallel, 2009). The piedmont plain is developed at the foot slope of the structural plateau with elevation ranging from 50 m to 100 m above sea level (Hammad, 1972); its surface is dissected by many Wadis. The structural tableland extends from the piedmont plain to the Qattara Depression; its elevation ranging from 100 m to 180 m above sea level (Fig. 2). Its northern edge is dissected by drainage lines which drain their water towards the Mediterranean Sea. The study area is located in two geomorphological units; the coastal plain unit and the piedmont plain unit.

The exposed rocks in the study area and its vicinities (Fig. 3) range in age from Middle Miocene to Holocene with a maximum thickness of about 200 m (Atwa, 1979).

- The Miocene sediments are represented by Marmarica Limestone that covers the most part of the northern plateau of the Western Desert (Said, 1962).
- The Pliocene sediments are limited on surface but in the subsurface they are concealed under younger formations.
- The Pleistocene sediments are differentiated into Oolitic limestone, Cardium limestone and Pink limestone; the Oolitic limestone covers the most parts of the northwestern coastal zone and it constitutes the main shallow aquifer in the study area.
- The Holocene deposits are represented by a variety of unconsolidated deposits formed from beach loose carbonate sand and alluvial deposits. The alluvial deposits are generally composed of quartz sand, silt and clay; they fill the shallow elongated depressions and channels of the drainage lines (El Sabri et al., 2011).

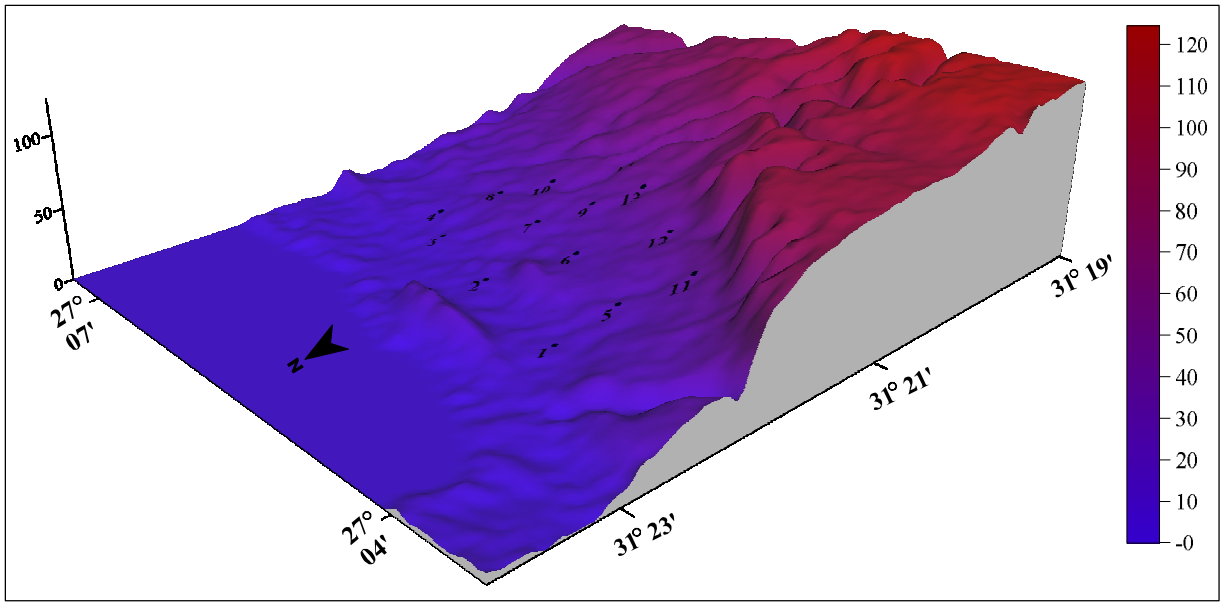

Fig. 2: Digital Elevation Model (DEM) of the study area.

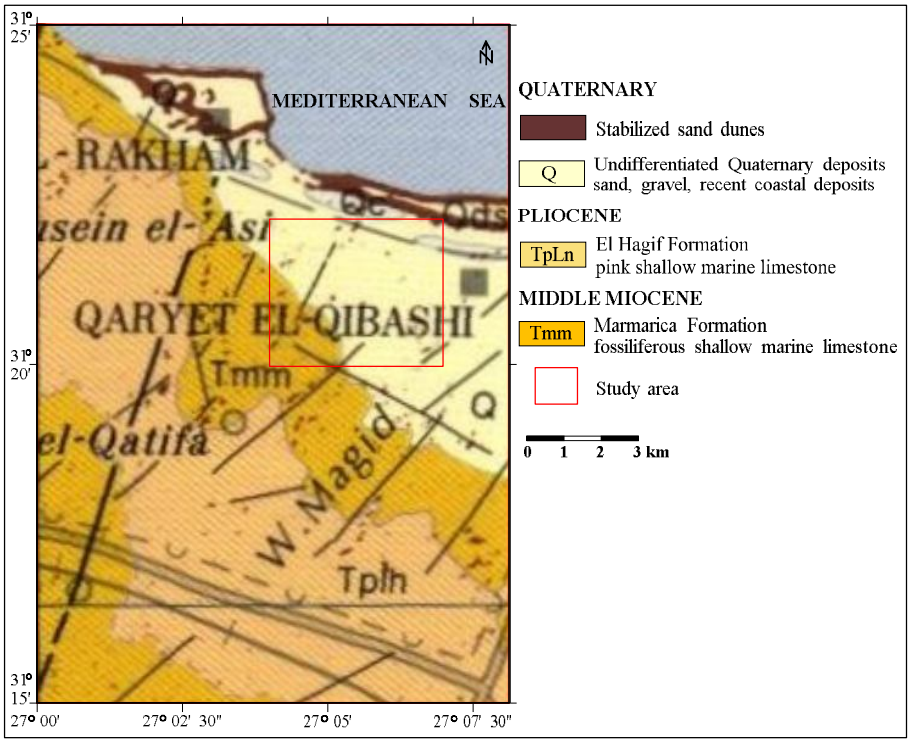

Fig. 3: Geological map of the study area (CONOCO, 1986).

Structurally, the study area is affected by several minor faults and joints. The faults have NE-SW trend that is accompanied with Aqaba trend and N-S trend which is detected only in the areas located southwest Matruh (Mohallel, 2009).

Hydrogeological setting of the northwestern coast of Egypt was the subject of many works (Abdel Mogheeth et al., 1978; Soliman, 2005 and Massoud et al., 2015). These studies concluded that there are three aquifers in the study area and its vicinities along the Northwestern Coast. These aquifers are the Alluvium aquifer (Holocene), Oolitic limestone aquifer (Pleistocene) and Fissured Marmarica limestone aquifer (Middle Miocene). The Holocene aquifer consists of unconsolidated calcareous sand which acts as a local reservoir that recharged directly from rainfall and accumulated surface runoff at the coastal area. Most of water drained to this aquifer percolates by gravity towards the lower Pleistocene aquifer. This aquifer is characterized by free water table condition; it exists at shallow depths at Matrouh area, it ranges from 1.5 m to 11 m and its salinities vary from 1380 ppm to 5800 ppm

(El Sabri et al., 2011). Pleistocene aquifer is considered as the main aquifer in the study area; it is composed of Oolitic limestone and the groundwater is occurred under free water table condition. It recharged from direct infiltration from the annual rainfall and percolation from the overlying Holocene aquifer; at Matrouh area depth to water ranges from 25m to 45m and its thickness varies from 10m to 75m. The salinity of this aquifer varies from 2770 ppm to 13800 ppm (El Sabri et al., 2011). Middle Miocene aquifer (Marmarica Formation) represents the deep aquifer in the northwestern coast, it is composed of limestone, dolomitic limestone intercalated with marl, clay and chalk. Joints and fractures play an important role in recharging of this aquifer (El Shazly, 1970).

3. MATERIALS AND METHODS

Surface geophysical survey includes Electric resistivity methods are extensively used for determining water bearing layers and mapping fresh/saline water interface which are essential information for management of the coastal aquifers. Lee and Song (2007) concluded that the extent of saline water intrusion is influenced by geological formations, hydraulic gradient, and rate of withdrawal of groundwater and its recharge. Seawater intrusion (SWI) in the coastal aquifers was the subject of many studies. These studies focused on mapping saltwater occurrence (Carrera et al., 2010 and Tran et al., 2012); corroboration of SWI models using geophysical data and groundwater dating (Goes et al., 2009 and Vandenbohede et al., 2011) and determine depths to brackish/salt water interface using Vertical Electrical Sounding and Electrical Resistivity Tomography (Barseem et al., 2014 and Eissa et al., 2016).

3-1- Vertical Electrical Sounding (VES)

In this work, fourteen Vertical Electrical Sounding (VES) stations were carried out in a form of a grid pattern to cover all the study area, Figure 1. This method was used to determine water bearing layers, their extension and depth to brackish/saline water interface. The conventional 4-electrodes Schlumberger array was used to acquire the apparent resistivity data with maximum current electrodes separation (AB) varies from 400 to 1000m. Field measurements were carried out by using Direct-Current resistivity meter "ABEM Terrameter SAS 1000". Some sounding stations were carried out nearby the existing wells to parameterize the geoelectrical measurements in view of the lithological succession and depth to water and hence control the interpretation of the acquired data. The acquired field curves were interpreted both qualitatively and quantitatively. Qualitative interpretation can give an idea about the resistivity of the subsurface layers (curve-type) and their aerial distribution which will help during the quantitative interpretation. Quantitative interpretation was done primary by manual (graphical) interpretation where the field curves with successive segments were matched with standard pre-calculated set of theoretical curves (Orellana and Mooney, 1966) with conjunction of auxiliary – point charts. This method gives a rough estimation about subsurface layering parameters (resistivity and thickness). To decrease the ambiguity during the qualitative interpretation, all available data from exist wells in form of thickness of layers, depth to water and total depth of well, previous studies and primary model from graphical interpretation were used to construct the initial model for IPI2Win software (2003), (Fig. 4).

3-2- Two-dimensional resistivity imaging technique (2-D)

Electrical Resistivity Tomography (ERT), including two-dimensional resistivity imaging technique (2-D), was used to accurate determine depth to water, thickness of water bearing layers and depth to the brackish/saline water interface. This technique was widely used to study groundwater occurrences in shallow limestone coastal aquifers because the huge contrast in resistivities between the saturated zone and the dry zone (Tassy et al., 2014 and Eissa et al., 2016).

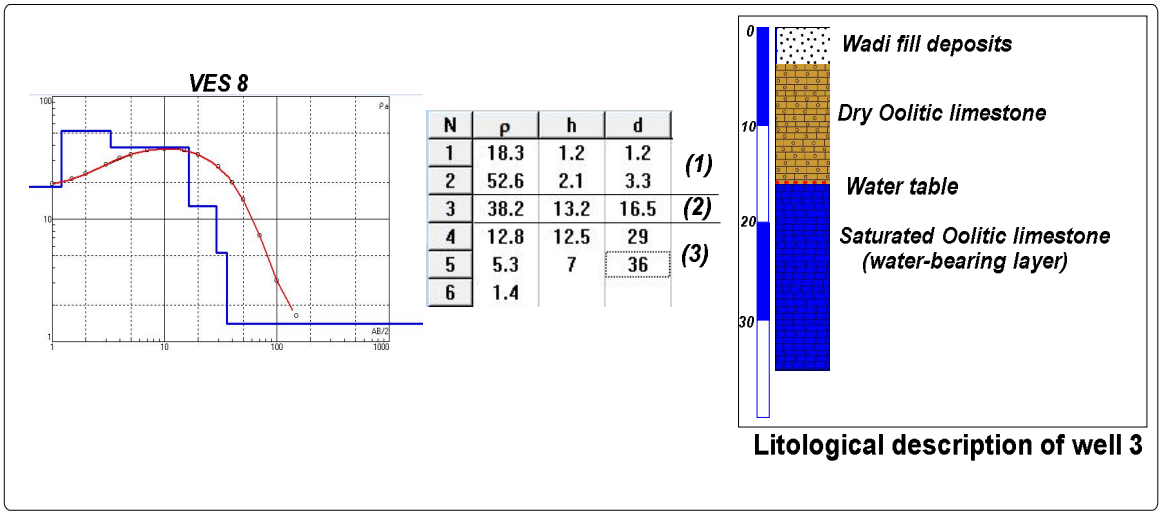

Fig. 4: Interpreted model of VES 8 and the lithological description of well 3.

Two imaging profiles (I-I' and II-II') were carried out in the study area at VES 3 and 10 respectively. These profiles extend from west to east perpendicular to the direction of sea water intrusion. Field measurements of these 2-D resistivity profiles were made by applying Wenner alpha configuration using ABEM LUND imaging system (Terrameter SAS 1000, electrode selector ES 10-64, and multi conductor cables). Field survey was carried out with a system where 31 steel electrodes are arranged along a line with a constant electrode spacing (a-spacing) at the same datum points and increasing this spacing by a multiplying factor (2, 3, 4, etc.) to increase depth of penetration along this profile. RES2DINV software (GEOTOMO, 2010) was used to invert the measured apparent resistivity data into a 2-D resistivity imaging model using the least-squares method (Loke and Barker, 1996a). This model demonstrated the low resistivity zone that represent water saturated layers and the high resistivity zone that represent the dry layers. The electrode spacing was selected to reach the required depth of investigation based on all available information about depth to water and ground elevation that are obtained from exist wells and DEM map of the study area. The electrode spacing was 7.0 m at profile I-I'; and its total length is 210m while this spacing was 12.5 m at profile II-II'; and its total length is 375m. The electrode spacing increased from north to south where depth to water and ground elevation are increased along this direction. The obtained results from VES method were used to correlate between the geoelectric layers and the geoelectric zones obtained from 2-D resistivity models.

3-3- Time Domain Electromagnetic sounding (TDEM)

Time Domain Electromagnetic sounding (TDEM) had proven successfully for mapping fresh/saline water interface where the conductivity of water bearing layer increases with increasing of water salinity that filling its pores. This method is used to determine changes in resistivity with depth due to its better vertical resolution and its lower sensitivity to geologic noise. Current pulses are sent through the transmitter loop laid on the ground surface, after cut off the current, the rapid decay of the current at the end of each pulse generates magnetic field diffuses into the stratified earth. Eddy currents induced by the time-varying magnetic field generate, in turn, secondary magnetic field in the electrically conductive stratified earth. The amplitude and rate of decay of these secondary fields are measured on the receiver loop and analyzed in terms of the variation in electrical resistivity with depth (Kontar and Ozorovich, 2006; Massoud et al., 2010 and Shaaban et al., 2016). Field data acquired with TEM-FAST 48HPC instrument with usage of ungrounded horizontal magnetic antennas in single loop configuration (square loop with 100m side length), one loop combines functions of the transmitter and receiver. Four TDEM soundings were carried out along one profile extends in NW-SE direction in the central part from the study area, at the same sounding site the measurements were repeated more than three times to obtain the best field curve (enhanced signal to noise ratio) suitable for processing and interpretation. TDEM sounding No. 4Q was measured adjacent to well 2 and VES 7 to aid in correlation and decrease the ambiguity during the interpretation of the acquired data. The acquired TDEM data in the form of apparent resistivity versus time were processed and inversed using 1X1D software (Interpex 2008) to obtain resistivity and thickness of the encountered layers, it based on Occam's inversion principle (Constable et al., 1987).

4. RESULTS AND DISCUSSION

4-1- Vertical Electric Sounding

4-1-1- Qualitative interpretation

Qualitative interpretation explains a general view on the lateral and vertical variations in the apparent resistivities along the area under consideration. It gives information about the number of layers, their continuity and reflects the degree of homogeneity between layers. The dominant curve type in the study area is HKQ with five or six layers, and the less common are KQ (VESes 1, 8 and 10) and QQ (VESes 3 and 5). All field curves are terminated by Q-type, they reflect homogeneity in the resistivities of the lower layers and their resistivities decrease with depth at the same station due to increase in water salinity. The upper layers have different curve types that reflect the heterogeneity between them where the ground surface is covered by wadi fill deposits or clay layer (Fig. 5).

4-1-2- Quantitative interpretation:

Quantitative interpretation of the Vertical Electric Soundings determines the geoelectric parameters that characterize each geoelectric layer (true resistivity and thickness) which are used to illustrate the vertical and spatial extensions of these layers, depth to water and depth to brackish/saline water interface. Based on the obtained results, the geoelectric succession in the study area consists of a group from geoelectric layers that are grouped into two main zones; dry zone (geoelectric layers A, B and C) and saturated zone (geoelectric layers D, E and F). Four geoelectric cross sections were constructed, they traverse the study area in NW–SE direction (A–A' and B–B') and NE–SW direction (C-C' and D-D') as illustrated in Figures 6 to 9. The following is a description of these geoelectrical layers from top downwards:

1- Geoelectric layer (A):

Geoelectric layer (A) represents the upper layer from the dry zone, it composed from wadi fill deposits such as silt, sand and rock fragments derived from the nearest tableland. The average resistivity of this layer varies from 13.0 Ohm.m at VES 7 to 114.6 Ohm.m at VES 3; the low resistivity value of this layer can be attributed to increase in its fine contents. Thickness of this layer attains 0.5m at VES 7 and 5m at VES 11. This layer not recorded at VESes 1, 4, 6 and 10 where the ground surface is covered by clay layer.

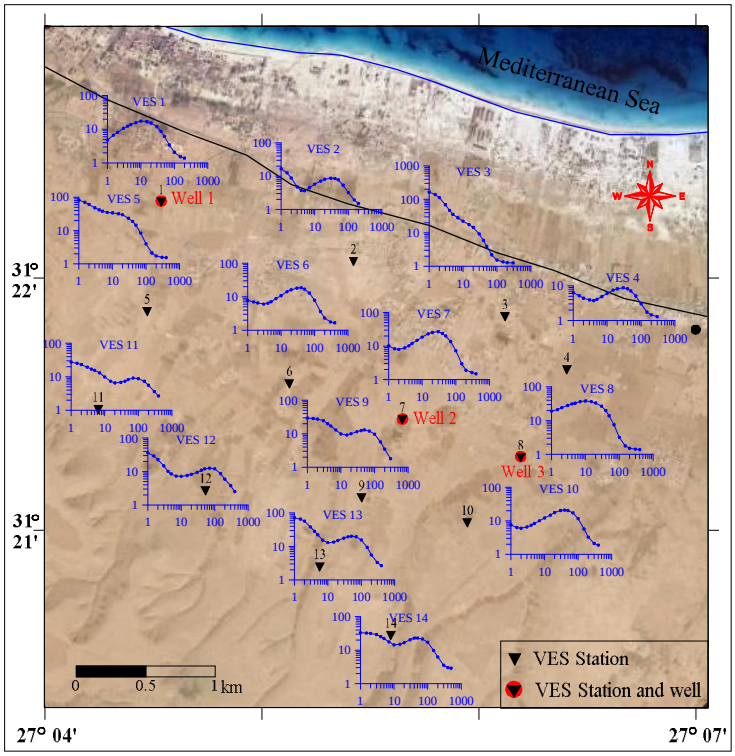

Fig. 5: Field curves distribution along the study area.

2- Geoelectric layer (B):

Geoelectric layer (B) represents clay deposits; its resistivity varies from 2.1 Ohm.m at VES 2 to 9.8 Ohm.m at VES 13 while its thickness is 0.5m at VES 1 and 16m at VES 12. This layer not detected at VESes 3, 5 and 8.

3- Geoelectric layer (C):

This layer is correlated with the upper dry part from the Oolitic limestone; it has resistivity values range from 23.0 Ohm.m at VES 4 to 42.8 Ohm.m at VES 7, and its thickness varies from 4.4m at VES 4 to 24.3m at VES 14. The thickness of this layer increases southward.

4- Geoelectric layer (D):

The saturated zone in the study area is represented by the saturated part from the Oolitic limestone. The geoelectric layer (D) is considered as the upper part from this zone; its resistivity varies from 11.0 Ohm.m at VES 1 to 15.9 Ohm.m at VES 10; in generally it decreases towards the North-West direction (Fig. 10). The thickness of this layer ranges from 11.2m at VES 3 to 18m at VES 11; it increases inland direction towards the South-West direction (Fig. 11). Depth to the upper surface of this layer which is considered as depth to water as it measured in the hand dug wells or it obtained from VES interpretation ranges from 6.75m at VES 3 to 34m at VES 14; it increases towards South-West direction due to increase in ground elevations along this direction (Fig. 12). The groundwater of this layer is occurred under free water table conditions and its measured salinity was 2790 ppm at well 2.

5- Geoelectric layer (E):

The middle part from the saturated zone is represented by the geoelectric layer (E); it has resistivity values range from 5.1 Ohm.m at VES 4 to 7.3 Ohm.m at VES 13 and its thickness varies from 3.5m at VES 3 to 17m at VES 14. The salinity of this layer is about 6272 ppm as it measured at well 3; the total depth of this well (33m) is sufficient to penetrate this layer that can be explained the increasing in salinity of this well.

6- Geoelectric layer (F):

This geoelectric layer represents the lower part from the saturated zone; its resistivity varies from 1.27 Ohm.m at VES 4 to 2.7 Ohm.m at VES 14; it increases southward. Depth to the upper boundary of this layer which represents depth to brackish/saline water interface range from 21.5m at VES 3 to 67m at VES 14; it increases inland direction (Fig. 13); while its lower boundary was not detected. The water content of this layer is affected by sea water contamination and it is not suitable for exploitation.

4-2- 2-D resistivity imaging profiles

The locations of the 2-D resistivity imaging profiles were selected at VES 3 and VES 10 where depth to water and depth to brackish/saline water interface are expected to be at shallow depths (VES 3) and became deeper southward (VES 10); also, they selected to avoid man made noises (structures and cables). The obtained 2-D resistivity model by the inversion algorithm performed with the RES2DINV software display variations in resistivity with depth; the resistivity values are controlled by the types of rocks and their fluid contents.

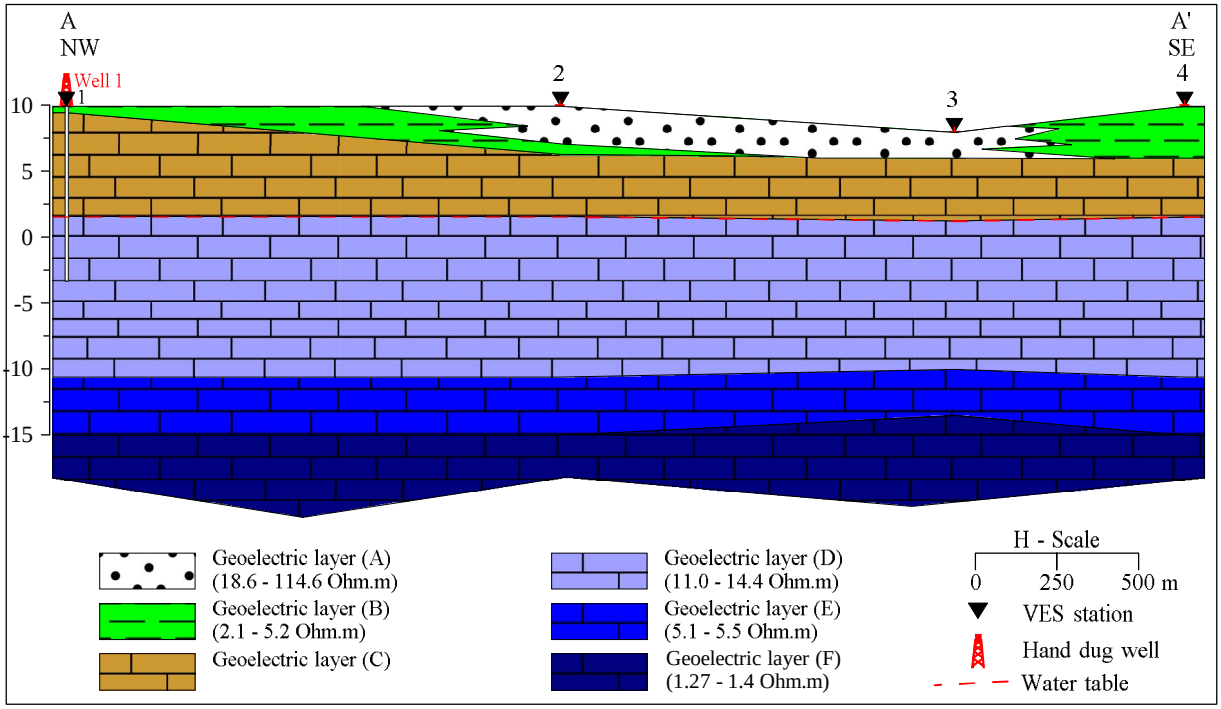

Fig. 6: Geoelectric cross section A-A'.

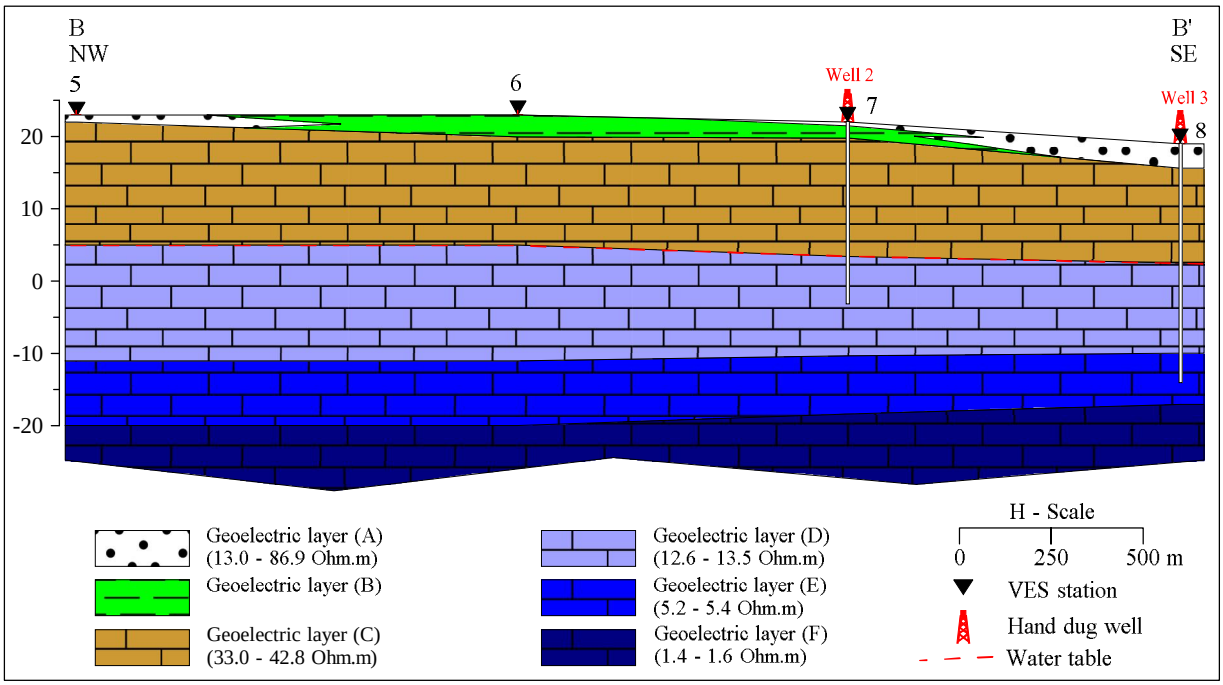

Fig. 7: Geoelectric cross section B-B'.

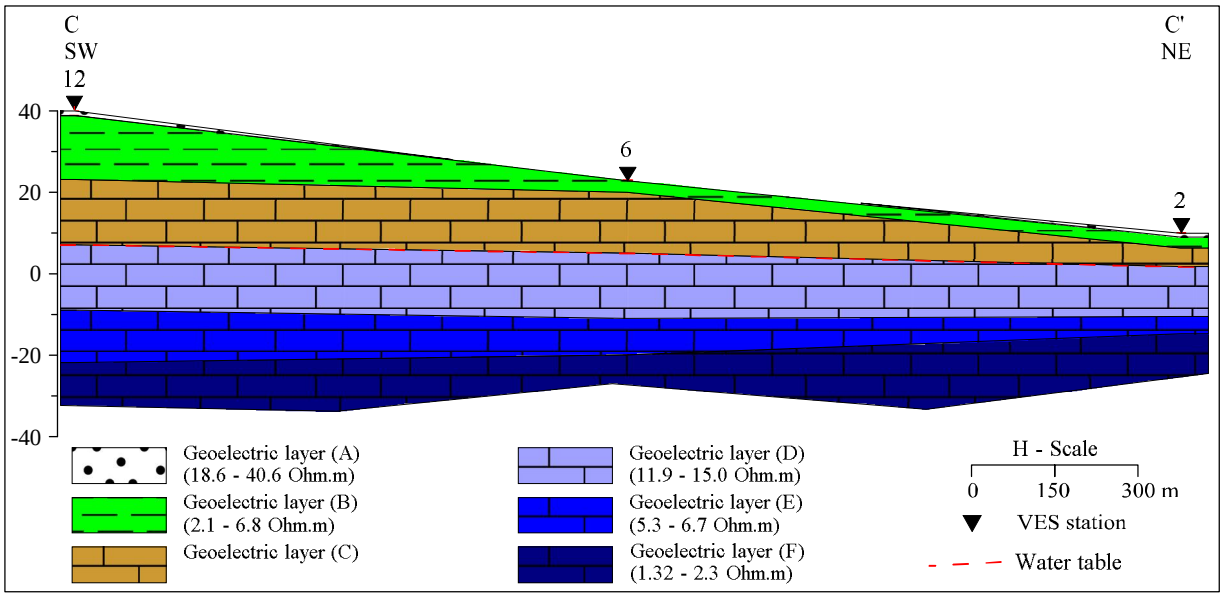

Fig. 8: Geoelectric cross section C-C'.

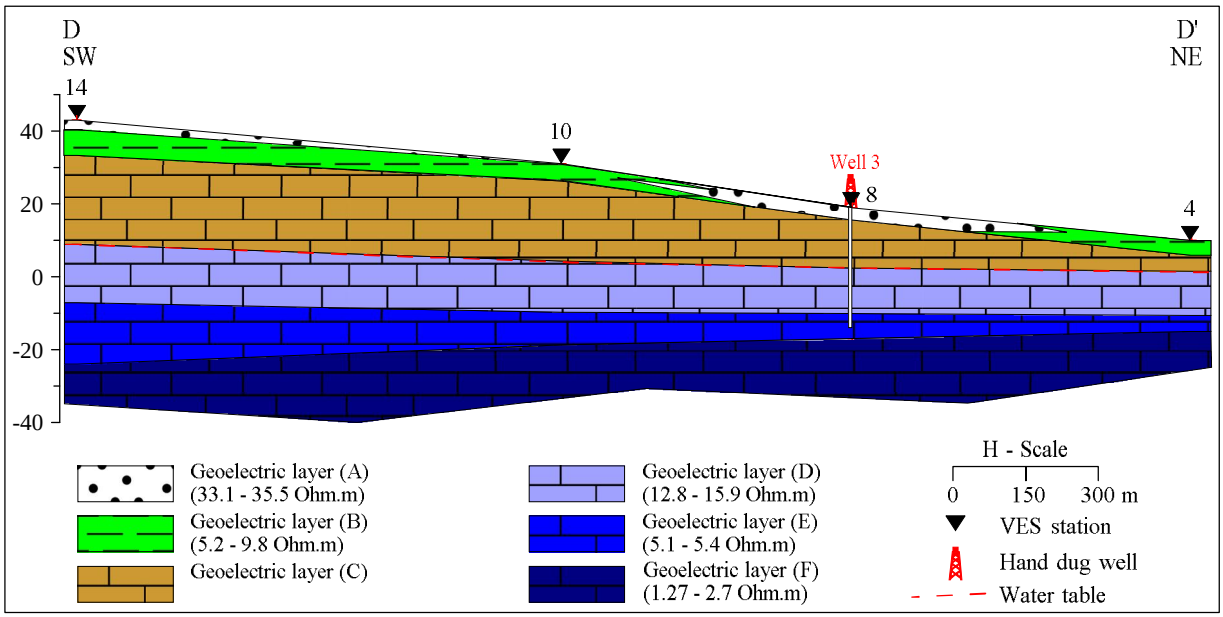

Fig. 9: Geoelectric cross section D-D'.

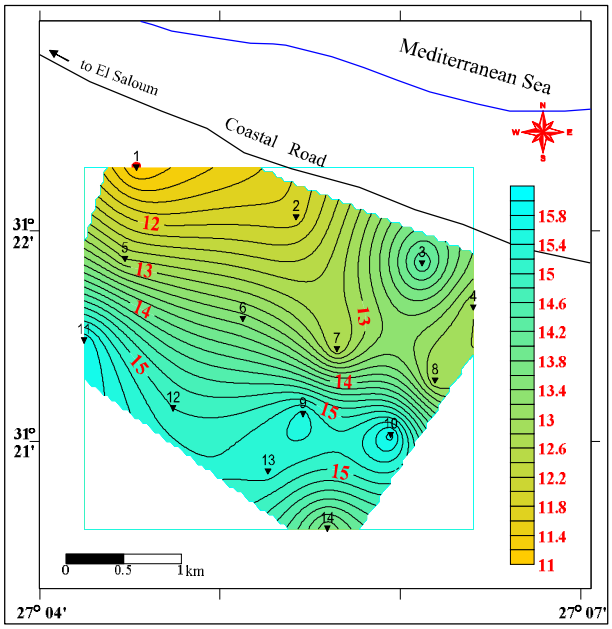

Fig. 10: Iso-resistivity contour map of the geoelectric layer D.

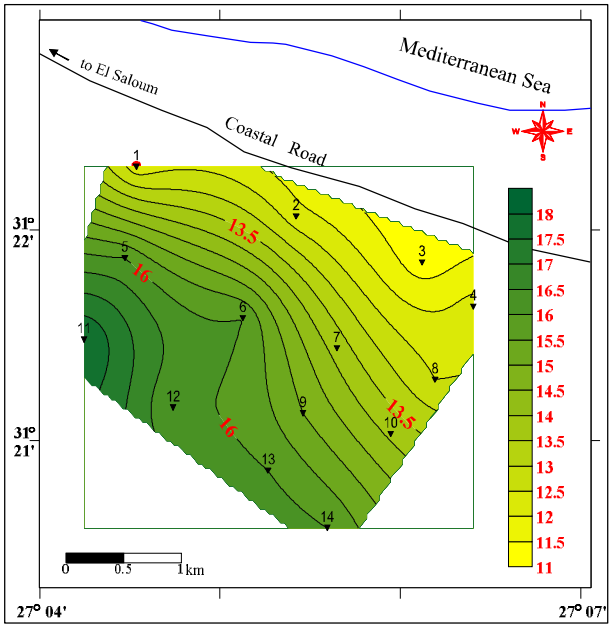

Fig. 11: Iso-pach map of the geoelectric layer D

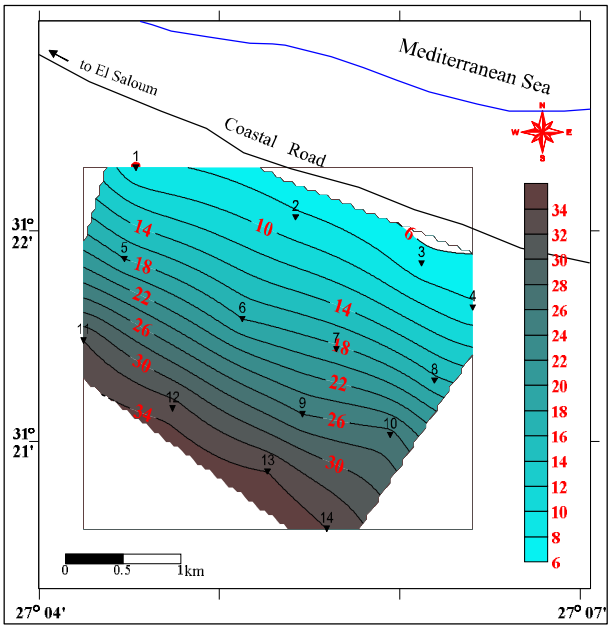

Fig. 12: Depth to the upper surface of the geoelectric layer D.

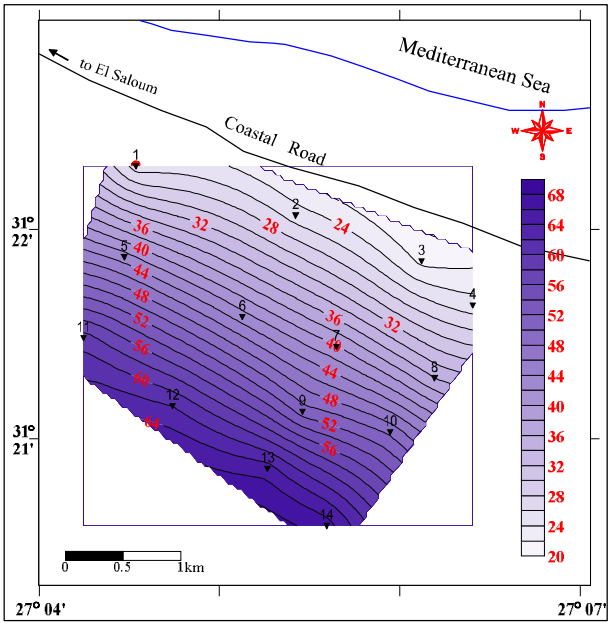

Fig. 13: Depth to brackish/saline water interface.

Surface Electrical Resistivity Tomography is a useful tool to determine sea water intrusion in the coastal aquifers due to its capability to discriminate between the presences of sea water, which strongly reduces the resistivity values, and the saturated fresh or brackish water layers. The inverse resistivity models of these 2-D profiles indicate that they are composed of two main zones; the upper dry zone and the lower saturated zone. The dry zone consists of thin sand or clay layers at the surface and the upper dry part from the Oolitic limestone beds. The lower zone consists of the saturated part from the Oolitic limestone beds. The following is a description of these profiles:

4-2-1- 2-D resistivity imaging profile I-I'

The inverse resistivity model of this profile (Fig. 14) indicates that the resistivity values of the dry zone vary from 14.0 Ohm.m to 29.68 Ohm.m and its thickness is about 6.75 m. The saturated zone can be divided into three layers; the upper one is correlated with the geoelectric layer D that obtained from VES interpretation; it represents the brackish water layer. The resistivity values of this layer vary from 5.0 Ohm.m to less than 14.0 Ohm.m, its resistivity decreases with depth due to increase in water salinity; and its thickness is about 11.7m. The middle layer is correlated with the geoelectric layer E, its resistivity decreases rapidly from less than 5.0 Ohm.m to 2.0 Ohm.m as a result of increasing in water salinity; its thickness is about 4.25m. The lower layer is correlated with the geoelectric layer F; its resistivity value ranges from 1.15 Ohm.m to less than 2.0 Ohm.m, its lower resistivity values can be attributed to contamination with sea water. The brackish/saline water interface is located at depth 22.7m from the ground surface.

4-2-2- 2-D resistivity imaging profile II-II'

The inverse resistivity model of this profile (Fig. 15) indicates that the resistivity values of the dry zone vary from 18.0 Ohm.m to 25.48 Ohm.m and its thickness is about 26.7m. The upper layer from the saturated zone (brackish water layer) has resistivity values vary from 5.0 Ohm.m to less than 18.0 Ohm.m, they decrease with depth due to increase in water salinity; its thickness is about 13.9m. The resistivity of the middle layer decreases rapidly from less than 5.0 Ohm.m to 3.0 Ohm.m as a result of increasing in water salinity; its thickness is about 9.0m. The lower layer (saline water layer) has resistivity value ranges from 1.68 Ohm.m to less than 3.0 Ohm.m, its lower resistivity values can be attributed to contamination with sea water. The brackish/saline water interface is located at depth 49.6m from the ground surface.

From the previous discussion it is clear that depth to water increases southward due to increase in ground elevation along this direction. Water table along these profiles decreases from (+ 4.3 m) at profile II-II' to (+ 1.25 m) at profile I-I' which indicates that the groundwater flow is from south to north. Brackish water layer is suitable for exploitation and its thickness increases southward. Depths to the brackish/saline water interface decreases from (- 14.7m) at profile I-I' to (- 18.6m) at profile II-II' which indicate that sea water intrusion is from north (Mediterranean Sea) to south (inland direction). In generally, resistivities of the saturated zone decrease with depth that can be attributed to increase in water salinity and the high conductivity of the saline water layer due to sea water intrusion can be used to discriminate it from other saturated layers.

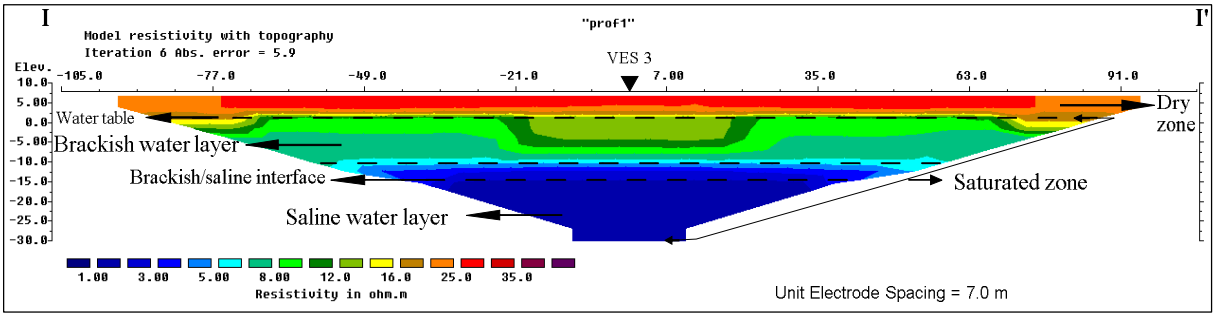

Fig. 14: 2-D resistivity imaging model I-I'.

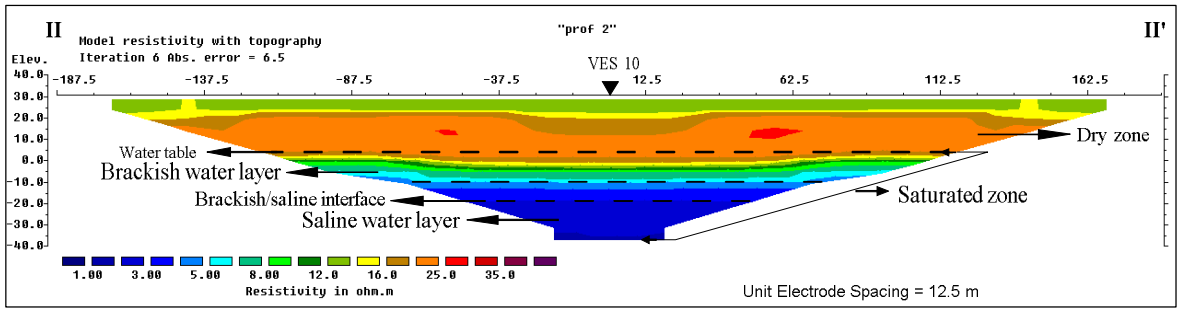

Fig. 15: 2-D resistivity imaging model II-II'.

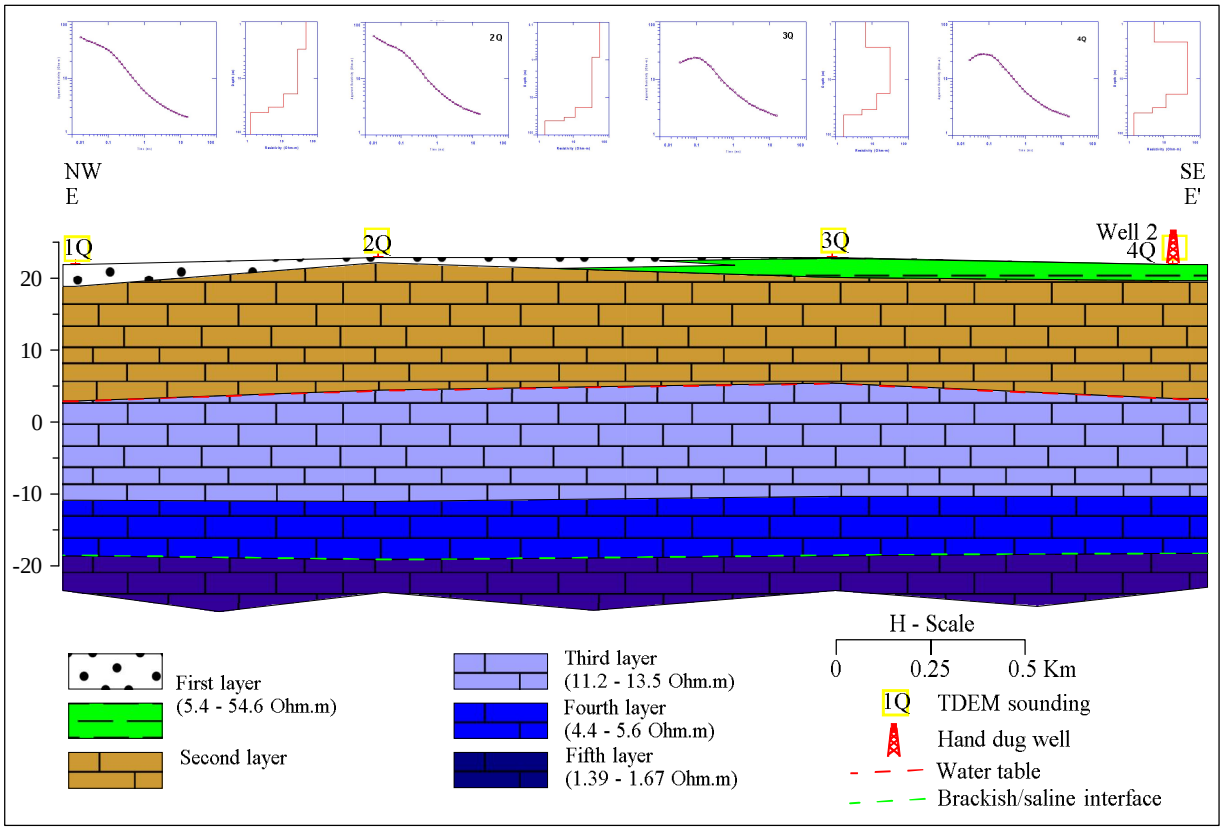

Fig. 16: TDEM profile along the central part from the study area.

4-3- TDEM Sounding

The first step for interpretation of the TDEM soundings based on constructing a model with minimum number of layers to best fit with the smoothed data, after that comparing the obtained results with the previous interpreted data from VES, 2-D and wells, additional layers can be added to the initial model to improve the interpretation. The vertical resistivity stratification of each TDEM sounding is used to construct a 2-D resistivity section E-E'; this section consists of five layers (Fig. 16).

The first layer is correlated with the geoelectric layers A and B that obtained from VES interpretation, it has resistivity values ranges from 54.6 Ohm.m at sounding 2Q to 5.4 Ohm.m at sounding 4Q; its thickness varies from 0.8m at sounding 2Q to 3.04m at sounding 1Q. This layer composed from wadi fill sediments in the western part from this section while in its eastern part it is composed from clay layer. The second layer is correlated with the geoelectric layer C; it has resistivity values range from 28.1 Ohm.m at sounding 1Q to 45.0 Ohm.m at sounding 4Q. Its thickness varies from 14.8m at sounding 3Q to 17.7m at sounding 2Q; it composed from dry Oolitic limestone layer. The third layer is correlated with the geoelectric layer D; its resistivity ranges from 11.2 Ohm.m at sounding 2Q to 13.5 Ohm.m at sounding 3Q. The thickness of this layer varies from 13.73m at sounding 4Q to 15.8m at sounding 3Q; it represents the brackish water bearing layer. The fourth layer is correlated with the geoelectric layer E; its resistivity ranges from 4.4 Ohm.m at sounding 1Q to 5.6 Ohm.m at sounding 2Q. The low resistivity values of this layer are contributed to increase in its water salinity; the thickness of this layer varies from 7.8m at sounding 1Q to 8.2m at sounding 3Q. The fifth layer is correlated with the geoelectric layer F; it represents the lower part from the Oolitic limestone aquifer contaminated with sea water. The resistivity value of this layer ranges from 1.39 Ohm.m at sounding 1Q to 1.67 Ohm.m at sounding 3Q. Depth to the upper surface of this layer is considered as depth to brackish/saline water interface; it ranges from 40.23m at sounding 4Q to 42.1m at sounding 2Q.

Porosity is an important property that characterizes the water bearing layers. Because of there is no pumping tests for the existing wells in the study area, it is difficult to calculate their hydraulic conductivity. So, the porosity of the coastal Oolitic limestone aquifer which is a fundamental property to evaluate it can be estimated from application of Archie's equation (1942). This equation expressed a relation between formation resistivity (bulk resistivity, ρ_0), resistivity of pore water (fluid resistivity, ρ_w) and formation porosity (ϕ).

$$\rho_0 = a\, \rho_w\, \phi^{-m} \quad \text{or} \quad \phi^m = a\, \rho_w / \rho_0$$

where; a and m are empirical constants specific to a formation, for soft formations as Oolitic limestone a = 0.81 and m = 2 (Humble formula- Schlumberger, 1972).

Resistivity of the water bearing layer is relied largely on its degree of saturation, its water salinity and

its porosity. TDEM soundings are accurately detect the brackish/saline water interface and hence determine the bulk resistivity of the water bearing layer below this interface to avoid the deviation from Archie's equation at low concentration of the total dissolved solids (Kafri and Goldman 2005, and Mahmoud 2011) . The reason for this is that surface conductance caused by the exchangeable ions of soil and rock complexes may become a major fraction of total ions (Kwader 1986). Fluid resistivity was determined using salinity/resistivity nomogram for a sea water sample (3.88×10^4 ppm at 20^oC). By replacing each variable with its value (a=0.81; m=2; ρ_w=0.19 Ohm.m and ρ_0 varies from 1.39 to 1.67 Ohm.m) the calculated porosity is founded to be ranges from 30% to 33%; this aquifer has an excellent porosity values.

5- CONCLUSIONS AND RECOMMENDATIONS

The study area is characterized by presence of Oolitic limestone aquifer; this aquifer is considered as a main source for irrigated water along the coastal region. The lower part from this aquifer is contaminated with sea water which decreases its efficiency. Vertical Electrical Soundings (VES) are used to determine water bearing layers and their spatial distribution, outline the brackish water bearing layer that is suitable for exploitation and to detect depth to brackish/saline water interface. The dominant curve type in the study area is HKQ-type, and all field curves are terminated by Q-type, they reflect homogeneity in the resistivities of the lower layers and their resistivities decrease with depth at the same station due to increase in water salinity. The obtained results from this tool indicate that the saturated zone is divided into three water bearing layers. The upper saturated layer (geoelectric layer D) represents the brackish water layer; it is suitable for exploitation where its salinity is low if compared with other middle and lower parts. The resistivity value of this layer varies from 11.0 Ohm.m to 15.9 Ohm.m; it decreases toward the NW direction. Its thickness ranges from 11.2m to 18.0m; it increases toward the SW direction. The middle saturated layer (geoelectric layer E) represents the transition layer between brackish water layer and saline water layer; its resistivity varies from 5.1 Ohm.m to 7.3 Ohm.m; it decreases downward at the same station due to increase in salinity with depth and its thickness ranges from 3.5m to 17.0m; it increases southward. The lower saturated layer (geoelectric layer F) has low resistivity values due to increase in its salinity as a result of sea water contamination; its resistivity varies from 1.27 Ohm.m to 2.7 Ohm.m; it increases toward the south direction. Depth to water in the study area ranges from 6.75m to 34.0m; it increases toward the SW direction. Groundwater flow is from south (inland) to north (Mediterranean Sea). Depth to brackish/saline water interface ranges from 21.5m to 67.0m; it increases southward; because sea water intrusion is from north to south.

2-D resistivity imaging technique is a useful tool to detect sea water intrusion in the coastal aquifers due to its capability to discriminate between the presences of sea water, which strongly reduces the resistivity values, and the saturated brackish water layers. The obtained results from the inverse resistivity models concluded that water table decreases from (+ 4.3 m) at profile II-II' to (+ 1.25 m) at profile I-I' which indicate that the groundwater flow is from south to north. Depths to the brackish/saline water interface decreases from (- 14.7m) at profile I-I' to (- 18.6m) at profile II-II' which indicate that sea water intrusion is from north (Mediterranean Sea) to south (inland direction). The high conductivity of the saline water layer due to sea water intrusion can be used to discriminate it from other saturated layers.

TDEM sounding is considered as an effective tool to determine brackish/saline interface where the conductivity of the water bearing layer increases with increasing water salinity. The brackish/saline water interface in the central part from the study area was accurately determined; it ranges from 40.23m to 42.1m. Bulk resistivity of the water bearing layer below this interface was determined to estimate the porosity of the coastal aquifer by applying Archie's equation. The calculated porosity ranges from 30% to 33%; so the Oolitic limestone aquifer has an excellent porosity values.

Based on the previous discussion the following can be recommended:

1- The best sites to drill new wells are at the locations of VES 11 and 12 because they have the maximum thickness of the brackish water layer and their resistivities are high if compared with other locations; their salinities are expected to be low where they are located near from the recharge area (tableland).

2- Monitoring wells must be drilled along the coastal area and piedmont plain to observe the extent of sea water intrusion inland direction.

3- Total depth of the new drilled wells must not be reached depth to brackish/saline water interface to avoid groundwater contamination with sea water.

4- Surface geophysical tools especially TDEM sounding must be carried out periodically in the piedmont plain to monitor sea water intrusion; where it sensitive to conductive saline water and need less array area if compared with other tools.

5- Safe yield must be determined accurately for each well to avoid deterioration of the Oolitic limestone aquifer.

REFERENCES

Abdel Mogheeth S.M., Taha A.A. and Hammad F.A. 1978. Hydrogeological Studies on the Tertiary and Quaternary Aquifers along the Coastal Zone of Egypt and Libya. Water Research Institute, Cairo, Internal Report.

Archie G.E. 1942. The electrical resistivity log as an aid in determining some reservoir characteristics. Trans. AIME. (146), 54-62.

Atwa S.M.M. 1979. Hydrogeology and hydrogeochemistry of the northern coast of Egypt. Ph.D. Thesis, Fac. Sci. Cairo Univ., Egypt, 162 p.

Barseem M.S., El Sayed A.N. and Youssef A.M. 2014. Impact of geologic setting on the groundwater occurrence in wadis El Sanab, Hashem, and Khrega using geoelectrical methods—northwestern coast, Egypt. Arab J Geosci (7), 5127–5139.

Carrera J., Hidalgo J. J. Slooten L. J. and Vazquez-Sune E. 2010. Computational and conceptual issues in the calibration of seawater intrusion models, Hydrogeology (18), 131–145.

CONOCO. 1986. Geological map of Egypt, Scale 1:500000: The Egyptian General Petroleum Corporation. Conoco Coral.

Constable S.C., Parker R.L. and Constable C.G. 1987. Occam's inversion—a practical algorithm for generating smooth models from EM sounding data. Geophysics (52), 289–300.

Eissa M. A., Mahmoud H. H., Stash O. S., El-Shiekh A. and Parker B. 2016. Geophysical and geochemical studies to delineate seawater intrusion in Bagoush area, Northwestern coast, Egypt. African Earth Sciences (121), 365-381.

El Sabri M. A., Masoud M. H. and Dahab K. A. 2011. Water budget assessment in some wadis west Matruh and possibilities of seawater intrusion. ISSN-1110-2527, Sedimentology of Egypt (19), 113 125.

El Shazly M.M. 1970. Contribution to the geochemistry of the groundwater in Mersa Matruh area (western Mediterranean coastal zone, Egypt). Bull. Inst. Desert, Cairo 20 (2), 289–299.

GEOTOMO (RES2DINV). 2010. Rapid 2-D Resistivity & IP inversion using the least-squares method. www.geoelectrical.com

Goes B.J.M., Essink G.H., Vernes R.W. and Sergi F. 2009. Estimating the depth of fresh and brackish groundwater in a predominantly saline region using geophysical and hydrological methods, Zeeland, the Netherlands. Near Surface Geophysics (7), 401–412.

Hammad F.A. 1972. The geology of soils and water resources in the area between Ras El Hekma and Ras Alam El Rum, western Mediterranean littoral zone, Egypt. Ph.D. Thesis, Fac. Sci. Alex Univ., Egypt, 225 p.

Interpex. 2008. 1X1D user's manual. Interpex Ltd., Colorado, USA.

IPI2Win. 2003. Resistivity Sounding Interpretation. Moscow State University. Version 3.0.1.a

Kafri U. and Goldman M. 2005. The use of the time domain electromagnetic method to delineate saline groundwater in granular and carbonate aquifers and to evaluate their porosity. Applied Geophysics (57), 167– 178.

Khalil M.A., Abbas A.M., Santos F., Massoud U. and Salah H. 2013. Application of VES and TDEM techniques to investigate sea water intrusion in Sidi Abdel Rahman area, northwestern coast of Egypt. Arab. J. Geosci. (6), 3093–3101.

Kontar A.E. and Ozorovich R.Y. 2006. Geo-electromagnetic survey of the fresh/salt water interface in the coastal southeastern Sicily. Continental Shelf Research (26), 843-851.

Kwader T. 1986. The use of geophysical logs for determining formation water quality. Ground water (24), 11-15.

Lee J.Y. and Song S.H. 2007. Evaluation of groundwater quality in coastal areas: implications for sustainable agriculture. Environmental Geology 52 (7), 1231–1242.

Loke M.H. and Barker R.D. 1996a. Rapid least-squares inversion of apparent resistivity pseudosections by a quasi-Newton method. Geophysical Prospecting (44), 131-152.

Mahmoud H.H. 2011. Contribution of geoelectrical survey methods in studying the condition of groundwater occurrence in El Alamein area – northwestern coast – Egypt. EGS Journal 9 (1), 181-189.

Massoud U., Soliman M., Taha A., Khozym A. and Sala H. 2015. 1D and 3D inversion of VES data to outline a fresh water zone floating over saline water body at the northwestern coast of Egypt. NRIAG Journal of Astronomy and Geophysics (4), 283–292.

Massoud U., Santos F., El Qady G., Atya M. and Soliman M. 2010. Identification of the shallow subsurface succession and investigation of the seawater invasion to the Quaternary aquifer at the northern part of El Qaa plain, Southern Sinai, Egypt by transient electromagnetic data. Geophys. Prospect. (58), 267–277.

Mohallel S. A. 2009. Hydrochemistry and Treatment of Groundwater in the area between Mersa Matruh and El Salloum, Egypt. Msc. thesis, Fac. Sci., Al-Azhar University, Egypt, 304 p.

Orellana E. and Mooney H. M. 1966. Master tables and curves for vertical electrical sounding over layered structures: Madrid, Interciencia, 150 p., 66 tables.

Said, R., 1962. The geology of Egypt: El Sevier, Publ. Co., Amestrdam, New York, 337 p.

Schlumberger. 1972. Schlumberger log interpretation charts.

Shaaban H., El-Qady G., Al-Sayed E., Ghazala H. and Taha A.I. 2016. Shallow groundwater investigation using time-domain electromagnetic (TEM) method at Itay El-Baroud, Nile Delta, Egypt. NRIAG Journal of Astronomy and Geophysics, http://dx.doi.org/10.1016/j.nrjag. 2016.05.004.

Soliman M.M. 2005. Environmental and Geophysical Assessment of the Ground and Subsurface Water Resources of Ras El-hekma Area, Northwestern Coast of Egypt. Ph.D. Ain Shams University, Fac. Sci., Cairo.

Soliman M.M., Massoud U., Mesbah H. and Ragab E. 2013. Mapping of sea water/fresh water interface at the northwestern coast of Egypt by 2-D resistivity imaging and transient electromagnetic soundings. Society of Exploration Geophysicists, SEG Annual Meeting, Houston, Texas, 1955–1960.

Tassy A., Maxwell M., Borgomano J., Arfib B., Fournier F., Gilli E. and Guglielmi Y. 2014. Electrical resistivity tomography (ERT) of a coastal carbonate aquifer (Port-Miou, SE France). Environ. Earth Sci. (712), 601-608.

Tran L.T., Larsen F., Pham N.Q., Christiansen A.V., Tran N., Vu H.V., Tran L.V., Hoang H.V, and Hinsby K. 2012. Origin and extent of fresh groundwater, salty paleowaters and recent saltwater intrusions in Red River flood plain aquifers, Vietnam, Hydrogeology (20), 1295–1313.

Vandenbohede A., Hinsby K., Courtens C. and Lebbe L. 2011. Flow and transport model of a polder area in the Belgian coastal plain: example of data integration. Hydrogeology (19), 1599–1615.